nature genetics

Target mimicry provides a new mechanism for regulation of microRNA activity

José Manuel Franco-Zorrilla[1], Adrián Valli[1], Marco Todesco[2], Isabel Mateos[1], María Isabel Puga[1], Ignacio Rubio-Somoza[2], Antonio Leyva[1], Detlef Weigel[2], Juan Antonio García[1] & Javier Paz-Ares[1]

MicroRNAs (miRNA) regulate key aspects of development and physiology in animals and plants. These regulatory RNAs act as guides of effector complexes to recognize specific mRNA sequences based on sequence complementarity, resulting in translational repression or site-specific cleavage[1,2]. In plants, most miRNA targets are cleaved and show almost perfect complementarity with the miRNAs around the cleavage site[3–8]. Here, we examined the non–protein coding gene *IPS1* (*INDUCED BY PHOSPHATE STARVATION1*) from *Arabidopsis thaliana*. *IPS1* contains a motif with sequence complementarity to the phosphate (P_i) starvation–induced miRNA miR-399, but the pairing is interrupted by a mismatched loop at the expected miRNA cleavage site. We show that *IPS1* RNA is not cleaved but instead sequesters miR-399. Thus, *IPS1* overexpression results in increased accumulation of the miR-399 target *PHO2* mRNA and, concomitantly, in reduced shoot P_i content[5–8]. Engineering of *IPS1* to be cleavable abolishes its inhibitory activity on miR-399. We coin the term 'target mimicry' to define this mechanism of inhibition of miRNA activity. Target mimicry can be generalized beyond the control of P_i homeostasis, as demonstrated using artificial target mimics.

In plants, phosphorous nutrition is one of the processes regulated by miRNAs[9–12]. P_i homeostasis is a critical determinant of growth performance and is subject to a complex regulatory system[13–15]. The P_i starvation–responsive miR-399 can guide the cleavage of *PHO2* RNA, which encodes an E2 ubiquitin conjugase–related protein that negatively affects shoot P_i content and P_i remobilization through an unknown mechanism[9–12]. In addition to *PHO2* mRNA, other RNAs containing a region of complementarity with miR-399 constitute a new class of P_i starvation–induced, non–protein coding RNAs, the *TPSI* family, originally described in tomato and represented in *A. thaliana* by several genes, including *IPS1* and *At4* (refs. 16–20). The functional importance of the region of miR-399 complementarity has been unknown. Here we show that *IPS1* is not cleaved by miR-399 but that *IPS1* can inhibit the effect of miR-399 on *PHO2* mRNA using a strategy based on target mimicry. This mechanism can be exploited to inhibit miRNAs other than miR-399.

IPS1, *At4* and other members of this family have only short, nonconserved ORFs, although an ORF that has the potential to encode a peptide of four amino acids, Met-Ala-Ile-Pro, is shared between *IPS1* and its close paralog *At4* (**Fig. 1a**)[17–20]. In contrast, a 23-nt-long motif has been conserved in members of this gene family from different plant species (**Fig. 1a** and **Supplementary Fig. 1a** online). This 23-nt nucleotide motif shows extensive sequence complementarity with miR-399. However, there are critical mismatches, including a bulge opposite positions 10–11 of the miRNA. Sequence complementarity in this region is required for miRNA-guided cleavage of mRNA targets[3–8].

To investigate the effect of miR-399 on *IPS1* mRNA, we examined transgenic plants overexpressing *IPS1* and miR-399, either alone or in combination. miR-399 overexpression did not result in any sign of *IPS1* RNA degradation (**Fig. 1b**), although it was effective in reducing *PHO2* mRNA accumulation. Notably, the effect of miR-399 on *PHO2* mRNA was greatly suppressed by simultaneous *IPS1* overexpression, suggesting that *IPS1* antagonizes the effects of miR-399. In agreement with previous reports on the negative effect of *PHO2* on shoot P_i content[9–12], the shoot P_i content of *IPS1*-overexpressing plants was lower than that in their counterparts lacking *IPS1* overexpression. We observed this effect both with and without miR-399 overexpression (**Fig. 1c**).

The fact that *IPS1* overexpression increased *PHO2* mRNA accumulation in plants not overexpressing miR-399, in which miR-399 was not even be detected on small RNA blots, led us to examine whether there was any indirect evidence for miR-399 activity in these plants. Analysis of miR-399 cleavage products of *PHO2* mRNA in plants not overexpressing miR-399 demonstrated there is indeed miR-399 activity in these plants and that this activity is reduced by *IPS1* overexpression (**Supplementary Fig. 2** online). These findings suggested that *IPS1* inhibits miR-399 activity, thereby resulting in increased *PHO2* mRNA accumulation and activity. In line with this, mapping the sequences of *IPS1* responsible for its effect on shoot P_i content and *PHO2* mRNA accumulation identified the region of complementarity

[1]Department of Plant Molecular Genetics, Centro Nacional de Biotecnología, Consejo Superior de Investigaciones Científicas (CSIC), Campus de Cantoblanco, 28049 Madrid, Spain. [2]Department of Molecular Biology, Max Planck Institute for Developmental Biology, 72076 Tübingen, Germany. Correspondence and requests for materials should be addressed to J.P.-A. (jpazares@cnb.uam.es).

Received 4 April; accepted 22 May; published online 22 July 2007; doi:10.1038/ng2079

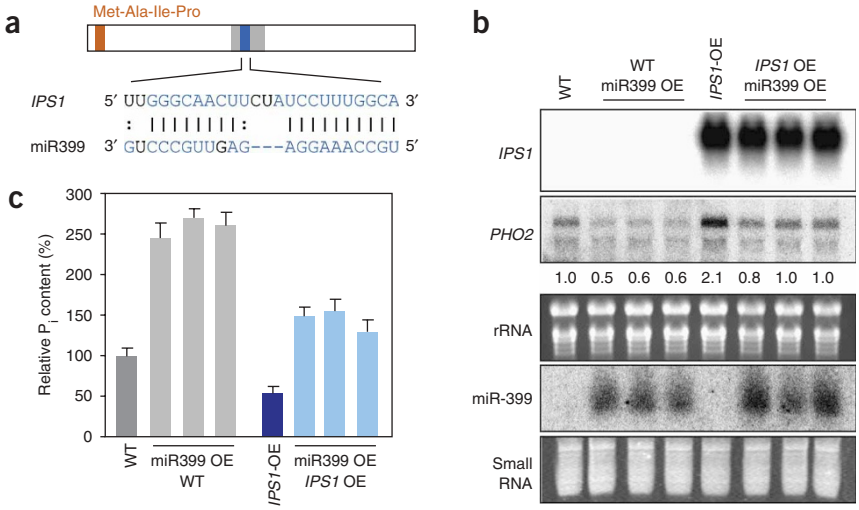

Figure 1 *IPS1* RNA resistance to miR-399–guided cleavage. (**a**) Diagram of *IPS1* highlighting the conserved miR-399 complementarity region (CR; blue shading). The region surrounding the CR (gray shading) and a short ORF that could encode the tetrapeptide Met-Ala-Ile-Pro (orange shading) is also related in sequence with *At4*, a close paralog gene from *A. thaliana*. The miR-399 family member shown is miR-399b, called 'miR-399' throughout the text, which has the highest complementarity to *IPS1*. Nucleotide positions invariant in more than 80% of all known *IPS1* and miR-399 family members are indicated in blue. (**b**,**c**) Counteracting effects of miR-399 and *IPS1* overexpression. Shown is RNA blot analysis of *PHO2*, *IPS1* and *miR-399* RNA accumulation (**b**) and shoot P_i content (**c**) of wild-type and *IPS1*-overexpressing (IPS1-OE) plants either overexpressing miR-399 (miR-399-OE, three independent lines) or not overexpressing miR-399, grown for 12 d under a P_i-rich regime. We observed significant differences (Student's *t*-test, $P < 0.001$) among all genotypes for shoot P_i content (error bars represent s.e.m.). Ethidium bromide staining of rRNA and small RNA is shown as a loading control for mRNA and miRNA hybridizations, respectively. Relative *PHO2 mRNA* accumulation in the different plant genotypes is indicated by numbers below each lane (normalized to accumulation in wild-type plants).

with miR-399 as crucial for the inhibitory effect of *IPS1* on miR-399 activity (**Supplementary Fig. 3** online).

We also tested the effects of overexpressing a close *IPS1* paralog, *At4*. As with *IPS1I*, *At4* overexpression also resulted in decreased shoot P_i accumulation (**Supplementary Fig. 4a** online). This finding suggests redundancy between *IPS1* and *At4* and possibly among the other *IPS1* family members, all of which are responsive to P_i starvation and contain a region of miR-399 complementarity (**Supplementary Fig. 1**). In line with the notion of functional redundancy is the observation that combined overexpression of *IPS1* and *At4* did not result in a further decrease of P_i accumulation (**Supplementary Fig. 4a**), which can be explained by *IPS1* and *At4* having very similar biological activity.

The effect of *At4* overexpression on shoot P_i accumulation is in agreement with the phenotypic consequences of inactivating *At4*, which results in a moderate but significant increase in shoot P_i content upon P_i starvation[20]. The modest size of the effect of *At4* inactivation is consistent with the presumed functional redundancy among the five members of the *IPS1* family in *A. thaliana*. The opposite type of effect of *At4* downregulation and overexpression argue against *At4* overexpression having nonphysiological effects. Instead, they support the notion that *IPS1* family members are *bona fide* riboregulators, rather than mere targets of miR-399. Consistent with the hypothesis that *IPS1* family members antagonize miR-399 activity, *PHO2* mutations masked the effects of *IPS1* or *At4* overexpression on P_i accumulation in shoots (**Supplementary Fig. 4a**).

We decided to further examine the hypothesis that *IPS1* and *At4* directly inhibits miR-399 activity and explore the mechanism of inhibition using transient expression of *IPS1*, miR-399 and a *PHO2:GFP* reporter in *Nicotiana benthamiana*. The expression cassettes were placed under the control of the 35S constitutive promoter to avoid feedback loops obscuring the interpretation of results. As expected, PHO2:GFP fluorescence and protein accumulation were reduced after overexpression of wild-type miR-399 (**Fig. 2a**,**b**). The direct interaction between *PHO2:GFP* and miR-399 was further confirmed by the observation that a form of *PHO2:GFP* with mutations in the miR-399-targeting motif was guided to cleavage by a form of miR-399 carrying the corresponding compensatory mutations (**Fig. 2a**,**c** and **Supplementary Fig. 5** online)[21]. The effect of miR-399 on *PHO2:GFP* was suppressed by simultaneous expression of *IPS1* (**Fig. 2b**), and a mutant form of *IPS1* with reduced complementarity to miR-399 did not affect miR-399–mediated silencing of *PHO2:GFP* (**Fig. 2a**,**d**). Finally, we reconstituted the interaction between *IPS1*, miR-399 and *PHO2* in a system in which complementary and compensatory mutations were introduced in all three components (**Fig. 2a**,**d**), also demonstrating that the *IPS1*–miR-399 interaction is direct. This suggests a model in which *IPS1* sequesters miR-399 through complementary interaction.

The resistance of *IPS1* mRNA to miRNA-guided degradation could be due to the presence of a mismatched loop in the miR-399 complementarity region that is predicted to impair miR-399-guided cleavage[3–8]. In this context, the sensitivity of miR-399 activity to *IPS1* overexpression could potentially be explained by *IPS1* RNA acting like a (noncleavable) pseudosubstrate inhibitor in classical enzyme reactions rather than acting as a competing substrate. In support of this hypothesis, the mismatched bases in *IPS1* are less highly conserved than the 5′ and 3′ positions that pair with miR-399, as the role of the mismatch is simply to prevent *IPS1* cleavage (**Supplementary Fig. 1a**,**b**).

To test directly whether noncleavability of *IPS1* is critical for its function, we performed transient expression assays to compare the wild-type form, *IPS1*, and a mutant form, *ips1 Perfect Match* (*ips1*^{PM}), in which perfect base-pairing with miR-399 is extended to the normally mismatched center of the miR-399–complementary motif. The *ips1*^{PM} mutation is predicted to render *IPS1* RNA susceptible to miR-399–guided cleavage. Whereas accumulation of wild-type *IPS1* RNA was unaffected by miR-399 overexpression, miR-399 caused degradation of *ips1*^{PM} RNA. Concomitantly, the inhibitory effect of *ips1*^{PM} on miR-399–mediated downregulation of *PHO2:GFP* was negligible (**Fig. 3**). It has recently been reported that a noncleavable miR-390 target site is *in vitro* a more efficient competitor for miR-390 compared with a cleavable substrate[22]. Our results agree with this finding and also suggest that cleavage of the miRNA competitor reduces its concentration to nonfunctional levels *in planta*.

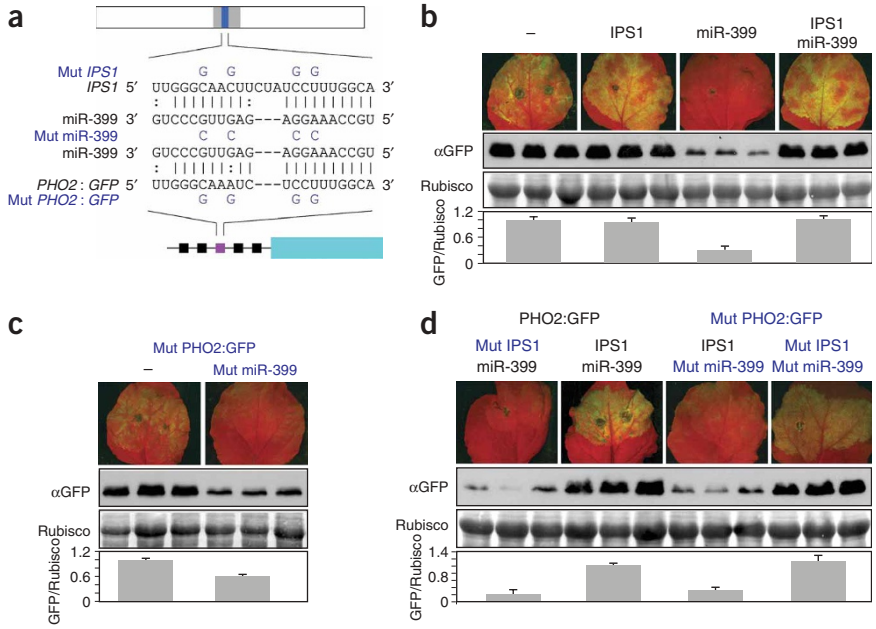

Figure 2 Effect of *IPS1* on miR-399–dependent *PHO2* accumulation requires base-pairing between *IPS1* and miR-399. (**a**) Constructs used in the agroinfiltration assays, driven by the 35S promoter of CaMV. *PHO2:GFP* contains the *PHO2* 5′ UTR with five potential miR-399 target sites and the ATG initiation codon fused to the *GFP* coding region. In the mutant ('Mut') *PHO2:GFP*, four point mutations were introduced into the third miR-399 target site, one of the two most frequently cleaved sites[5]. The *IPS1* construct is depicted as in **Figure 1**. Mutant *IPS1* has mutations at positions within the miR-399 complementarity region, equivalent to those in mutant *PHO2:GFP*. Mutant miR-399 has mutations that restore base pairing with those in mutant *PHO2:GFP* and mutant *IPS1*. (**b**–**d**) Transient expression assays in *N. benthamiana*, monitoring *PHO2:GFP* either by fluorescence microscopy or by protein blot. '–' indicates control agroinfiltration experiments using strains with an empty vector. Ponceau staining showing the Rubisco band is shown as loading control. Relative PHO2:GFP accumulation in the different agroinfiltration assays is indicated in bar graphs below each panel. Error bars represent s.e.m. from three replicates.

That the mismatched loop in *IPS1* is critical for its function is consistent with previous reports that overexpression of miRNA targets with cleavable target sites has few, if any phenotypic effects, in general. In contrast, overexpression of miRNA targets with disrupted target sites that are no longer accessible to miRNA-guided cleavage often leads to marked phenotypes[3]. If miRNA targets with intact target sites were generally able to sequester miRNAs, one would expect that overexpression of unmodified miRNA targets would have similar effects as overexpression of miRNA targets with disrupted target sites.

Two examples of miRNAs where overexpression of the wild-type targets has few consequences are miR-156, which targets a series of *SPL* genes[23], and miR-319, which has complementary motifs in a series of *TCP* and *MYB* genes[24]. To demonstrate that target mimicry provides insight into general principles of miRNA function, we modified the miR-399–complementary motif of *IPS1* to mimic target sites for miR-156 ('MIM156') and miR-319 ('MIM319') (**Fig. 4a**). In contrast to the weak effects previously reported for overexpression of cleavable miR-156 or miR-319 target sites, we found that plants overexpressing MIM156 and MIM319 had marked phenotypes. MIM156-overexpressing plants had very long plastochrons, flowering at the same time as control plants, but with a much smaller number of leaves (3.4 ± 1.3 rosette leaves, $n = 81$, primary transformants) than in controls (10.1 ± 0.8, $n = 30$), which is the opposite of the phenotype seen in plants with increased miR-156b expression[6]. Likewise, MIM319-overexpressing plants had smaller leaves (**Fig. 4b**), which is the opposite of what is seen in plants overexpressing miR-319a[24]. In addition, stamen development was arrested. In line with the phenotypic effects, several targets of miR-156 and miR-319 showed an increase in expression in different tissues of transgenic plants overexpressing these mimics (**Fig. 4c**,**d**). There was variation in the magnitude of the effect of artificial mimicry, which we attribute to differential expression of the target mimics in different transgenic plants. All phenotypes were confirmed in following generations.

In conclusion, target mimicry, consisting of a noncleavable RNA that forms a nonproductive interaction with a complementary

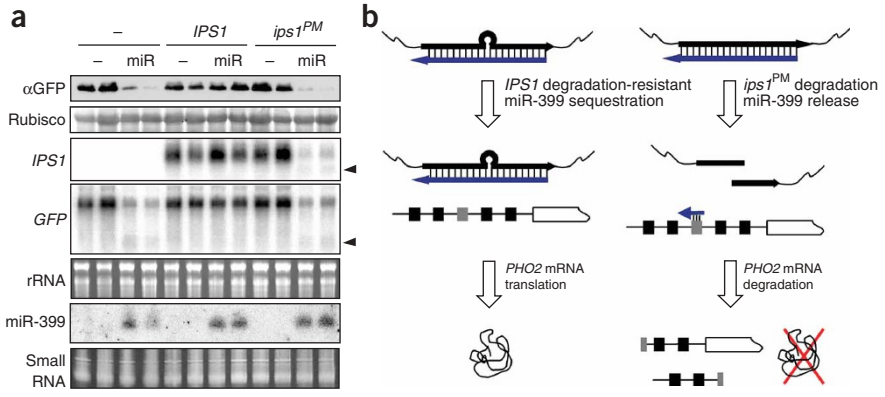

Figure 3 Efficient *IPS1* inhibition of miR-399 requires *IPS1* RNA resistance to miR-399–guided cleavage. (**a**) Agroinfiltration assays in which the *Agrobacterium* strain harboring the *PHO2:GFP* reporter gene was inoculated in combination with a mock strain or a miR-399 strain, alone or with strains harboring wild-type *IPS1* or a mutant derivative (*ips1*^{PM}). *ips1*^{PM} is a mutant derivative of *IPS1* with full sequence complementarity to miR-399 in the complementary region. RNA expression was examined by blot analysis. Ethidium bromide staining of rRNA and small RNA is shown as a loading control for mRNA and miRNA hybridizations, respectively. Arrowheads indicate RNA molecules shorter than the full-length transcript, indicative of miRNA-guided cleavage. (**b**) Model for miRNA inhibition by target mimicry. The target mimic, represented here by *IPS1*, requires miRNA recognition (that is, sequence complementarity) as well as resistance to miRNA-guided cleavage. A degradation-sensitive substrate does not show any significant miRNA inhibitory activity, as measured on a second substrate (*PHO2*).

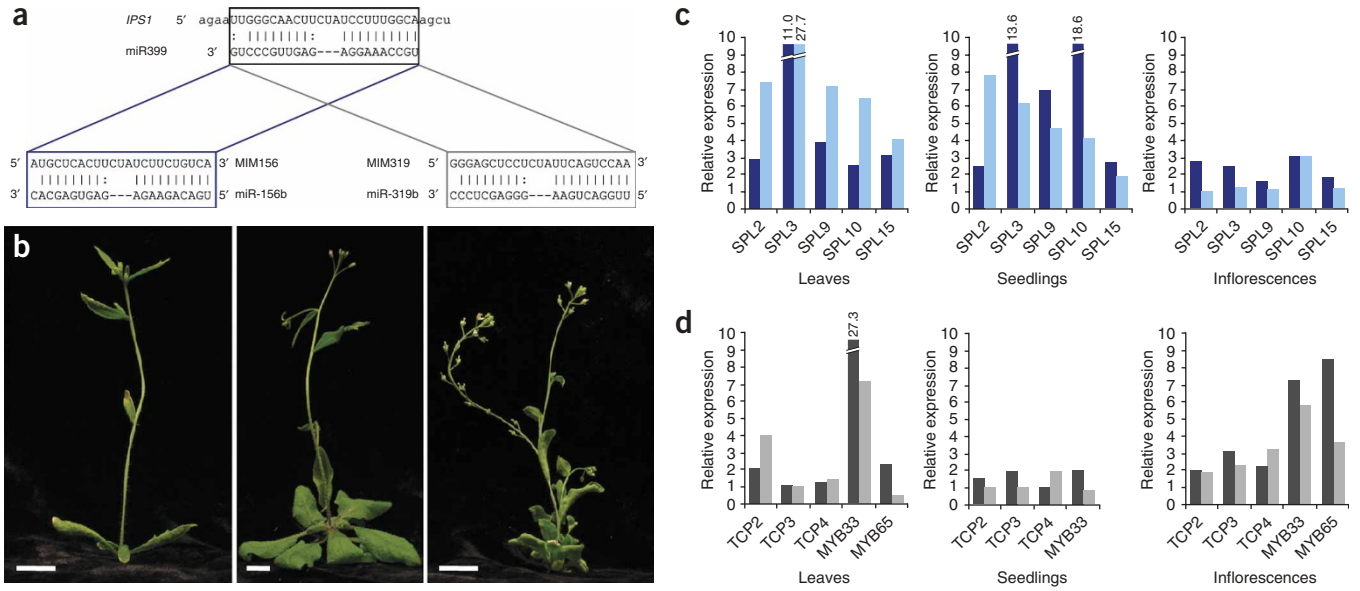

Figure 4 Artificial target mimics. (**a**) Design strategy for changing the miR-399 complementary sequence in *IPS1* into a mimic sequence for miR-156 ('MIM156') and miR-319 ('MIM319') families. (**b**) Phenotypes of 25-d-old primary transformants constitutively expressing MIM156 (left) and MIM319 (right) compared with a wild-type plant (center, shown at smaller scale). Scale bars = 0.5 cm. (**c**,**d**) Real-time RT-PCR analysis of selected targets of miR-156 (**c**) and miR-319 (**d**). Expression in different tissues is shown as a multiple of expression in control plants, in two independent experiments.

miRNA, provides a new strategy that can be used to inhibit the activity of specific miRNAs. We propose that *IPS1* family members represent an example of natural target mimicry. In this proposed situation, the P_i starvation responsiveness of both miR-399 and *IPS1* family members along with their antagonistic roles provides a fine-tuning mechanism for the control of P_i starvation responses and homeostasis. This principle, in which elicitation of a signal is closely followed by attenuation of the signal, is common to many signal transduction pathways that rely on regulatory protein molecules. We are not surprised that RNA-based signaling uses a similar mechanism. It will be interesting to determine how often this general principle is used in nature and whether endogenous target mimics are normally restricted to noncoding RNAs. In addition, because many occur in large families, reverse genetic analyses of plant miRNAs have been difficult. Artificial target mimicry provides a new tool for the functional analysis of plant miRNAs.

METHODS

Plants and P_i measurements. *Arabidopsis thaliana* (L.) Heynh (ecotype Col-0) plants were grown as described[25]. For P_i starvation treatments, plants where grown for 7 d in complete medium and were then transferred to medium lacking P_i for 3–4 additional days before harvesting[25]. Cellular P_i was measured according to the method of Ames[26] in plants grown for 12 d in complete medium. Data represent mean ± s.e.m. from three replicates and three independent experiments.

Binary constructs and plant transformation. *IPS1* and *At4* constructs were made from almost full-size cDNA[19]. cDNA was excised with *Not*I, blunt-ended with the Klenow fragment of DNA polymerase I and cloned in the *Sma*I site of pROK2 downstream of the 35S promoter of cauliflower mosaic virus[27]. The 5′ UTR region of *PHO2* and miR-399b were obtained by PCR from genomic DNA. Details on the constructs can be found in **Supplementary Methods** and **Supplementary Table 1** online. All binary constructs were introduced into the C58 strain of *Agrobacterium tumefaciens*, and *A. thaliana* plants were transformed as described[28]. *Agrobacterium*-mediated transient expression assays in *N. benthamiana* plants were carried out as described[29]. All experiments were performed twice in five independent plants; representative data are shown.

RNA blotting. RNA was extracted with the RNAwiz reagent (Ambion), and 15 μg RNA was loaded in each lane. RNA electrophoresis, transfer to nylon membranes and hybridization were performed using standard procedures, as described[25]. Details on the probes can be found in **Supplementary Methods** and **Supplementary Table 1**. Small RNAs (30 μg) were separated on 15% polyacrylamide gels containing 8 M urea. A DNA antisense probe corresponding to miR-399b was labeled with T4 polynucleotide kinase (Roche) and 50 μCi of γ-^{32}P-ATP. Hybridizations were performed at 37 °C overnight in 50% formamide/5× SSC/5× Denhardt's solution/0.5% SDS.

GFP analyses. Immunochemical detection of GFP and imaging were performed as described[30].

Construction and analysis of transgenic artificial mimicry plants. Artificial mimicry sequences were engineered into the *IPS1* gene, cloned into pGEM-T Easy vector (Promega) and used as PCR template (see **Supplementary Methods** for details). Total RNA was extracted from pooled primary transformants using TRIzol Reagent (Invitrogen), either from 10-d-old seedlings (12–15 individuals per pool) or from leaves and inflorescences from 30-d-old plants (5–7 individuals per pool). Reverse transcription was performed with the RevertAid First Strand cDNA Synthesis Kit (Fermentas), using as starting material 2 μg of total RNA treated with DNase I (Fermentas). PCR (see **Supplementary Table 1** for oligonucleotides) was carried out in presence of SYBR green (Invitrogen) and was monitored in real time with the Opticon Continuous Fluorescence Detection System (MJR).

Accession codes. GenBank CoreNucleotide (all are mRNA sequences; MIPS codes are given in parentheses): *IPS1* (ref. 19), AF236376 (At3g09922); *At4* (ref. 17), AF055372 (At5g03545); *At4-1* (ref. 20), AY536062; *At4-2* (ref. 20), AY334555; *At4-3*, AI995459; *PHO2* (refs. 9–12), NM–179887 (At2g33770). miRBase: miR-399b precursor, MI0001021 (refs. 9–12); mature miR-399b[9–12], MIMAT0000952; mature miR-156b[23], MIMAT0000167; mature miR-319b[24], MIMAT0000512.

Note: Supplementary information is available on the Nature Genetics website.

ACKNOWLEDGMENTS

We thank C. Aragoncillo, C. Castresana, M. Crespi, C. Martin, S. Prat, R. Solano and H. Vaucheret for reading the manuscript and C. Mark for editorial assistance. Technical assistance by M.J. Benito is acknowledged. We also thank the European Arabidopsis Stock Centre (NASC) stock centre for providing plant material. A.V. is supported by a fellowship from CSIC–Fondo Social Europeo (FSE), and I.M. and I.R.-S. by fellowships from the Spanish Ministry of Science and Education (MEC). Primary support for this work was provided by grants from the European Union, Comunidad de Madrid and MEC. Additional support came from the Marie Curie Research Training Network SY-STEM (M.T.) and the Max Planck Society (D.W.).

AUTHOR CONTRIBUTIONS

J.M.F.-Z. was responsible for experiments in **Figure 1** and **Supplementary Figures 1–5** and prepared constructs and performed RNA blot analysis corresponding to **Figures 2–3**. A.V. performed transient expression assays in **Figures 2–3** and **Supplementary Figure 5**. M.I.P. and I.M. prepared constructs and performed Pi measurements shown in **Supplementary Figure 3**. M.T. and I.R.-S. performed the artificial mimicry experiments shown in **Figure 4**. D.W. supervised the artificial mimicry experiments in **Figure 4**. J.A.G. supervised the transient expression assays in **Figures 2–3** and **Supplementary Figure 5** and contributed to discussion of other experiments. J.P.-A. supervised this study and wrote the manuscript. A.L. contributed to supervision and general discussion. J.A.G., D.W., J.M.F.-Z. and all other authors commented on the manuscript.

COMPETING INTERESTS STATEMENT

The authors declare no competing financial interests.

Published online at http://www.nature.com/naturegenetics
Reprints and permissions information is available online at http://npg.nature.com/reprintsandpermissions

1. He, L. & Hannon, G.J. MicroRNAs: small RNAs with a big role in gene regulation. *Nat. Rev. Genet.* **5**, 522–531 (2004).
2. Bartel, D.P. MicroRNAs: genomics, biogenesis, mechanism, and function. *Cell* **116**, 281–297 (2004).
3. Jones-Rhoades, M.W., Bartel, D.P. & Bartel, B. MicroRNAs and their regulatory roles in Plants. *Annu. Rev. Plant Biol.* **38**, 19–53 (2006).
4. Mallory, A.P. & Vaucheret, H. Functions of microRNAs and related small RNAs in plants. *Nat. Genet.* **38**, S31–S36 (2006).
5. Allen, E., Xie, Z., Gustafson, A.M. & Carrington, J.C. microRNA-directed phasing during trans-acting siRNA biogenesis in plants. *Cell* **121**, 207–221 (2005).
6. Schwab, R. *et al.* Specific effects of microRNAs on the plant transcriptome. *Dev. Cell* **8**, 517–527 (2005).
7. Vazquez, F. *et al.* Endogenous trans-acting siRNAs regulate the accumulation of *Arabidopsis* mRNAs. *Mol. Cell* **16**, 69–79 (2004).
8. Simón-Mateo, C. & García, J.A. MicroRNA-guided processing impairs Plum pox virus replication, but the virus readily evolves to escape this silencing mechanism. *J. Virol.* **80**, 2429–2436 (2006).
9. Fujii, H., Chiou, T.J., Lin, S.I., Aung, K. & Zhu, J.K. A miRNA involved in phosphate-starvation response in *Arabidopsis*. *Curr. Biol.* **15**, 2038–2043 (2005).
10. Chiou, T.J. *et al.* Regulation of phosphate homeostasis by microRNA in *Arabidopsis*. *Plant Cell* **18**, 412–421 (2006).
11. Aung, K. *et al. pho2*, a phosphate overaccumulator, is caused by a nonsense mutation in a microRNA399 target gene. *Plant Physiol.* **141**, 1000–1011 (2006).
12. Bari, R., Datt Pant, B., Stitt, M. & Scheible, W.R. PHO2, MicroRNA399, and PHR1 define a phosphate-signaling pathway in plants. *Plant Physiol.* **141**, 988–999 (2006).
13. Poirier, Y. & Bucher, M. Phosphate transport and homeostasis in *Arabidopsis*. in *The Arabidopsis Book* (eds. Sommerville, C.R. & Meyerowitz, E.M.) (American Society of Plant Biologists, Rockville, Maryland, 2002).
14. Ticconi, C.A. & Abel, S. Short on phosphate: plant surveillance and countermeasures. *Trends Plant Sci.* **9**, 548–555 (2004).
15. Franco-Zorrilla, J.M. *et al.* The transcriptional control of plant responses to phosphate limitation. *J. Exp. Bot.* **55**, 285–293 (2004).
16. Burleigh, S.H. & Harrison, M.J. A novel gene whose expression in *Medicago truncatula* roots is suppressed in response to colonization by vesicular-arbuscular mycorrhizal (VAM) fungi and to phosphate nutrition. *Plant Mol. Biol.* **34**, 199–208 (1997).
17. Burleigh, S.H. & Harrison, M.J. The down regulation of *Mt4*-like genes by phosphate fertilization occurs systemically and involves phosphate translocation to the shoots. *Plant Physiol.* **119**, 241–248 (1999).
18. Liu, C., Muchhal, U.S. & Raghothama, K.G. Differential expression of *TPSI1*, a phosphate starvation-induced gene in tomato. *Plant Mol. Biol.* **33**, 867–874 (1997).
19. Martín, A.C. *et al.* Influence of cytokinins on the expression of phosphate starvation responsive genes in *Arabidopsis*. *Plant J.* **24**, 559–567 (2000).
20. Shin, H., Shin, H.S., Chen, R. & Harrison, M.J. Loss of *At4* function impacts phosphate distribution between the roots and the shoots during phosphate starvation. *Plant J.* **45**, 712–726 (2006).
21. Vaucheret, H., Vazquez, F., Crete, P. & Bartel, D.P. The action of ARGONAUTE1 in the miRNA pathway and its regulation by the miRNA pathway are crucial for plant development. *Genes Dev.* **18**, 1187–1197 (2004).
22. Axtell, M.J., Rajagopalan, R. & Bartel, D.P. A two-hit trigger for siRNA biogenesis in plants. *Cell* **127**, 565–577 (2006).
23. Wu, G. & Poethig, R.S. Temporal regulation of shoot development in *Arabidopsis thaliana* by miR156 and its target SPL3. *Development* **133**, 3539–3547 (2006).
24. Palatnik, J.F. *et al.* Control of leaf morphogenesis by microRNAs. *Nature* **425**, 257–263 (2003).
25. Franco-Zorrilla, J.M., Martin, A.C., Leyva, A. & Paz-Ares, J. Interaction between phosphate-starvation, sugar, and cytokinin signaling in *Arabidopsis* and the roles of cytokinin receptors CRE1/AHK4 and AHK3. *Plant Physiol.* **138**, 847–857 (2005).
26. Ames, B.N. Assay of inorganic phosphate, total phosphate and phosphatases. *Methods Enzymol.* **8**, 115–118 (1966).
27. Baulcombe, D.C., Saunders, G.R., Bevan, M.W., Mayo, M.A. & Harrison, B.D. Expression of biologically active viral satellite RNA from the nuclear genome of transformed plants. *Nature* **321**, 446–449 (1986).
28. Bechtold, N., Ellis, J. & Pelletier, G. *In planta Agrobacterium* mediated gene transfer by infiltration of adult *Arabidopsis thaliana* plants. *CR Acad. Sci. Paris Life Sci.* **316**, 15–18 (1993).
29. Jiménez, I., López, L., Alamillo, J.M., Valli, A. & García, J.A. Identification of a plum pox virus CI-interacting protein from chloroplast that has a negative effect in virus infection. *Mol. Plant Microb. Interact.* **19**, 350–358 (2006).
30. González, E., Solano, R., Rubio, V., Leyva, A. & Paz-Ares, J. PHOSPHATE TRANSPORTER TRAFFIC FACILITATOR1 is a plant-specific SEC12-related protein that enables the endoplasmic reticulum exit of a high-affinity phosphate transporter in *Arabidopsis*. *Plant Cell* **17**, 3500–3512 (2005).